JOURNAL OF GEOPHYSICAL RESEARCH, VOL. 106, NO. D24, PAGES 33,543–33,550, DECEMBER 27, 2001

Intercomparison of BOREAS northern and southern study area surface fluxes in 1994

Alan G. Barr,[1] Alan K. Betts,[2] T. A. Black,[3] J. H. McCaughey,[4] and C. D. Smith[1]

Abstract. Sensible and latent heat fluxes from the Boreal Ecosystem and Atmosphere Study (BOREAS) tower flux sites in 1994 are analyzed over both diurnal and seasonal cycles. We compare and contrast the southern and northern study areas and the behavior of five different land covers. For each land cover the evaporative fractions and surface conductances to water vapor are higher in the south than in the north, with the ranking from largest to smallest: aspen, fen, black spruce and jack pine. The conifer and, particularly, the jack pine sites show the greatest stomatal control of transpiration, as the vapor pressure deficit increases from morning to afternoon and as the soil dries during periods with low precipitation. The relation between surface conductance and the Priestley-Taylor coefficient α is consistent between southern and northern study areas but varies among land covers. The aspen and fen sites have higher α values than the landscape mean, and the mature conifer sites have lower α values than the landscape mean. We attribute the differences to the impact of spatial heterogeneity at the landscape scale.

1. Introduction

The processes that govern the exchanges of heat and water vapor between natural ecosystems and the atmosphere play a key role in the global climate system. These processes are partially under the control of surface vegetation via canopy composition and structure, leaf area index and plant ecophysiology, specifically, the interactions between stomata (i.e., leaf or canopy conductance) and the controlling environmental variables, including light, temperature, humidity, and soil moisture. From a climatic perspective the surface exchange is mainly controlled by surface available energy (net radiation minus storage) and its partition into sensible and latent heat flux over both diurnal and seasonal cycles.

Few field experiments have attempted to characterize these exchanges at the landscape scale. The Boreal Ecosystem-Atmosphere Study (BOREAS) was one such experiment, designed to evaluate the role of boreal forests in the global climate system and in global change [*Sellers et al.*, 1995, 1997]. In this paper, we summarize the water and heat flux data from the BOREAS 1994 field campaigns over both diurnal and seasonal cycles. We also compare and contrast the BOREAS northern and southern study areas and the five land covers represented by the BOREAS tower flux sites.

[1]Climate Research Branch, Meteorological Service of Canada, Saskatoon, Saskatchewan, Canada.

[2]Atmospheric Research, Pittsford, Vermont.

[3]Faculty of Agricultural Sciences, University of British Columbia, Vancouver, British Columbia, Canada.

[4]Department of Geography, Queens University, Kingston, Ontario, Canada.

Paper number 2001JD900070.
0148-0227/01/2001JD900070$09.00

2. Data Sets and Processing

This study analyzes tower flux data from the 1994 field phase of BOREAS, collected at nine sites (Table 1) between May 24 and September 19. The BOREAS southern and northern study areas (SSA and NSA, respectively) had paired sites for four land covers: mature (old) black spruce (wet conifer) (SOBS and NOBS), mature jack pine (dry conifer) (SOJP and NOJP), young jack pine (SYJP and NYJP) and fen (Sfen and Nfen). In addition, the southern study area had a mature aspen (deciduous) site (SOA).

Sensible and latent heat flux densities (H and λE) were measured every half hour by the eddy covariance method at all sites, with subtle site-to-site differences in instrumentation and signal processing [*Newcomer et al.*, 2000]. Supporting meteorological measurements included solar and net radiation (R_s and R_n, respectively), air temperature (T_a), relative humidity (RH), vapor pressure deficit (D, defined as the difference between saturation vapor pressure at air temperature and ambient vapor pressure), and wind speed (u), again with some site-to-site differences in instrumentation [*Newcomer et al.*, 2000].

2.1. Evaporative Fraction and Priestley-Taylor Alpha

We will use two derived variables to describe the partition of available energy into the sensible and latent heat fluxes, the evaporative fraction (EF) and the Priestley-Taylor coefficient α [*Priestley and Taylor*, 1972]. The values for EF and α were estimated for each half hour as

$$\mathrm{EF} = \frac{\lambda E}{(H + \lambda E)} \tag{1}$$

and

$$\alpha = \frac{(s+\gamma)\lambda E}{s(H + \lambda E)}, \tag{2}$$

where γ is the psychrometric constant and s is the derivative of saturation vapor pressure with respect to temperature. Our formulation and use of α differs from that of *Priestley and*

Table 1. BOREAS Tower Flux Sites Used In This Study

Site	Latitude, °N	Longitude, °W	BOREAS Principal Investigator [a]	Reference
Southern mature aspen (SOA)	53.63	-106.20	T.A. Black (TF-1); G. den Hartog (TF-2)	*Black et al.* [1996]
Southern mature black spruce (SOBS)	53.98	-105.12	P.J. Jarvis (TF-9)	*Jarvis et al.* [1997]
Southern mature jack pine (SOJP)	53.92	-104.69	D D. Baldocchi (TF-5)	*Baldocchi et al.* [1997]
Southern young jack pine (SYJP)	53.88	-104.65	D E. Anderson (TF-4)	*Anderson et al.* [1995]
Southern fen (Sfen)	53.80	-104.62	S B. Verma (TF-11)	*Suyker et al.* [1997]
Northern mature black spruce (NOBS)	55.88	-98.48	S C. Wofsy (TF-3)	*Goulden et al.* [1997]
Northern mature jack pine (NOJP)	55.93	-98.62	D R. Fitzjarrald (TF-8)	*Fitzjarrald et al.* [1995
Northern young jack pine (NYJP)	55.90	-98.29	J.H. McCaughey (TF-10)	*McCaughey et al.* [1997]
Northern fen (Nfen)	55.91	-98.42	D.E. Jelinski (TF-10)	*Lafleur et al.* [1997]

[a] TF denotes the BOREAS Tower Flux group.

Taylor [1972] in two respects. First, to avoid the issue of energy balance nonclosure we have substituted ($H + \lambda E$) for (R_n - Q_s), where Q_s is the sum of the minor energy balance terms (section 2.2). If we assume that the measured Bowen ratio ($H/\lambda E$) is correct, this substitution in both (1) and (2) has the same effect as adjusting H and λE to force energy balance closure (section 2.2). Second, unlike Priestley and Taylor's original energy-limited concept and definition, our use of α, which is diagnostic rather than predictive, encompasses both energy-limited and soil water-limited conditions.

2.2. Energy Balance Closure

The surface energy balance may be written as

$$R_n - Q_s = H + \lambda E \tag{3}$$

and

$$Q_s = Q_s + Q_b + Q_a + Q_v + Q_c\,, \tag{4}$$

where Q_g is the ground heat flux, Q_b is the rate of aboveground biomass heat storage, Q_a and Q_v are the rates of sensible and latent heat storage, respectively, in the air layer below the eddy flux measurement level, and Q_c is the photosynthetic energy flux. Four of the nine tower flux sites had complete measurements of the terms in (4): SOA, SOJP, NYJP and Nfen. At sites where Q_s was not measured, Q_s was estimated as $f(R_n)$, using a fourth-order polynomial with coefficients fit to data from the most similar site where Q_s was measured (e.g., Nfen for Sfen, NYJP for SYJP, SOJP for NOJP, SOJP for SOBS, and SOJP for NOBS). These estimates are only approximate but are the best available. However, even with the measured or estimated Q_s, the surface energy balance (equation 3) does not close. Energy imbalances are common in eddy covariance studies [see, e.g., *Barr et al.*, 1994; *Twine et al.*, 2000], but their cause is uncertain and may vary among sites. Possible causes include eddy covariance measurement errors or limitations, violation of eddy covariance assumptions [*Mahrt*, 1998] and errors in the measurement of R_n - Q_s.

Therefore, before calculating the surface conductance to water vapor (equation 5), we resolved the energy imbalance in (3) by adjusting H and λE to force energy balance closure, assuming, as in the calculation of EF and α above, that the measured Bowen ratio was correct [*Barr et al.*, 1994; *Blanken et al.*, 1997; *Twine et al.*, 2000]. We will denote the closure-adjusted values of H and λE as H^* and λE^*, respectively. The mean adjustment to half-hourly H and λE varied among sites, from near zero at SOBS to +4% at NOBS, +7% at SYJP, +9% at SOJP, +15% at SOA, +19% at NYJP, +27% at Sfen, +31% at Nfen, and +38% at NOJP. The closure adjustments were applied only when the Bowen ratio was well defined [*Ohmura*, 1982]. The adjustments were applied consistently at all sites and, in the absence of additional information, provide the most reasonable solution to the closure problem [*Twine et al.*, 2000]. Still, the large, unexplained differences in closure among sites are a cause for concern. The large energy imbalances at some sites (the fens, in particular) may be due in part to the underestimation of Q_s.

2.3. Surface Conductance

The surface conductance to water vapor g_s was calculated from the closure–adjusted value for λE (λE^*) using the inverted form of the Penman-Monteith combination equation [*Monteith*, 1981]:

$$g_s = \frac{\gamma \lambda E^*}{[s(R_n - Q_s - \lambda E^*) - \gamma \lambda E^*]/\, g_a + \rho c_p D}, \tag{5}$$

where g_a is the aerodynamic conductance to heat and water vapor, ρ is the density of air, c_p is the specific heat of air, and D is the vapor pressure deficit. The value for s in (5) was estimated at the mean of surface temperature and air temperature, where surface temperature (T_s) was computed as

$$T_s = T_a + \frac{H^*}{\rho c_p g_a}. \tag{6}$$

The value for g_a was calculated, following *Thom* [1972] and *Verma* [1989], as

$$g_a = \frac{u_*^2}{u + B^{-1} u_*}, \tag{7}$$

where u_* is the friction velocity and B^{-1}, the dimensionless sublayer Stanton number, was set to 2 (forest) or 4 (fen) [*Thom*, 1972; *Wu et al.*, 2000]. The value for u_* was estimated on the basis of the stability corrected logarithmic wind profile [see, e.g., *Brutsaert*, 1984], with the zero-plane displacement and the roughness length for momentum set to 64% and 13% of the canopy height, respectively. At the six sites where measurements of u_* were available, there was general agreement between the measured and derived values for u_*, with a mean difference of 0.11 m s^{-1} and a root-mean-square difference of 0.21 m s^{-1}. We used the derived values for u_* in

(7) to be consistent among sites, but the effect of using derived or measured u_* was small.

It is difficult to estimate error limits for EF (equation 1), α (equation 2) and g_s (equation 5), because we lack independent estimates of the separate errors in H and λE. It is possible that the errors in EF, α, and g_s are smallest for sites with small energy imbalances (in sequence from smallest to largest: SOBS, NOBS, SYJP, SOJP, SOA, and NYJP) and largest for sites with large energy imbalances (the fens and NOJP), but this is only tentative because the actual cause of the energy imbalance is not known. It is equally possible that by using (1a) and (2) to skirt the closure issue, we have effectively minimized the errors in EF and α related to energy balance nonclosure.

2.4. Filling Gaps in Data

Appendix A gives more details on how we filled gaps in the flux and conductance data. Briefly, gaps in H^* and λE^* were filled using equations (3) and (A3), with missing values for g_s in (A3) estimated using an empirical function (equation A1) of R_s, D, and T_a. Gaps in meteorological data were filled using linear regression models and data from nearby BOREAS mesonet or tower flux sites. Gaps in Q_s were filled with modeled values, estimated as $f(R_n)$ using a fourth-order polynomial with site-specific coefficients fit to the entire period.

3. Comparison of SSA and NSA Sites in the 1994 Growing Season

3.1. Seasonal Cycle of Evaporative Fraction

Figure 1 shows the seasonal cycles of (1) air temperature and relative humidity (10-day averages), (2) evaporative fraction (10-day averages), and (3) precipitation (10-day totals) for the SSA and NSA flux sites. Values of T_a and RH are averaged over all sites. For precipitation we show a single average in the NSA and two values in the south; one for the SSA aspen site and the other for an average representative of the other SSA sites, which are in a cluster ~100 km to the east-north-east of the aspen site. Note the difference in early summer precipitation between the two. There is a cool wet period, with high RH in early summer (with more precipitation in the SSA than in the NSA), followed by a warmer, drier period, with little rainfall, toward the end of July. Among the conifer sites, EF at the jack pine sites, which have permeable sandy soils, is more sensitive to precipitation, while EF at the black spruce sites, where the water table is high and the organic soil has high water retention, varies much less with precipitation and has a slight upward trend over the season. EF is much higher at the deciduous aspen site, increasing rapidly with leaf out in late May, and at the fen sites, where the vegetation is also mostly deciduous. The aspen and fen sites show a midsummer EF peak, following the early summer rains. Figure 1 also shows that mean

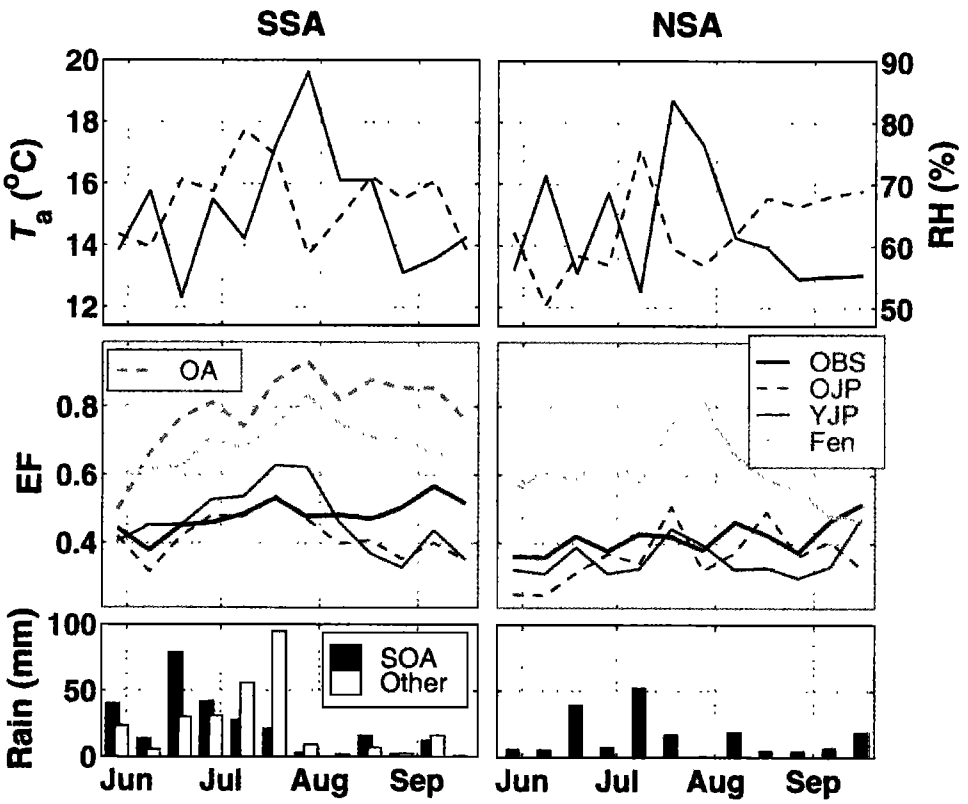

Figure 1. Seasonal variation in (top) air temperature T_a (solid lines) and relative humidity RH (dashed lines), (middle) evaporative fraction EF, and (bottom) rainfall from BOREAS tower flux sites in the southern study area SSA and northern study area NSA during the 1994 growing season. The data are 10-day averages for T_a, RH, and EF and 10-day totals for rainfall. Before calculating EF, we first averaged the 10-day fluxes. The EF line style denoted for each land cover type is the same for sites in the SSA and NSA. Abbreviations are as follows: OA, mature aspen; OBS, mature black spruce; OJP, mature jack pine; and YJP, young jack pine.

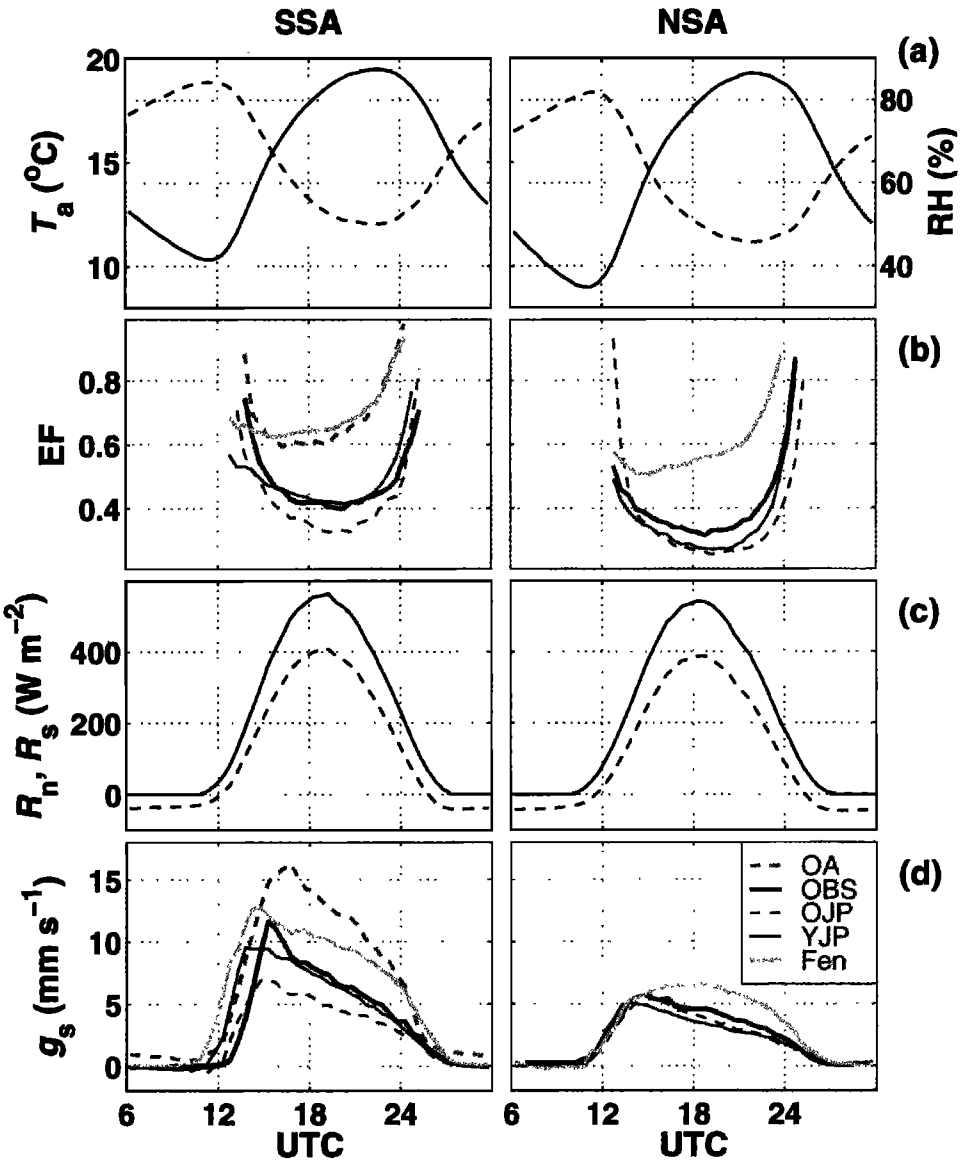

Figure 2. Diurnal variation in (a) air temperature T_a (solid lines) and relative humidity RH (dashed lines), (b) evaporative fraction EF, (c) solar radiation R_s (solid lines) and net radiation R_n (dashed lines), and (d) surface conductance to water vapor g_s from BOREAS tower flux sites in the SSA and NSA, averaged between May 24 and September 19, 1994. We first averaged the fluxes by time of day before calculating EF. The mean surface conductance was calculated from measured data only (i.e., with no gap filling) after excluding values below the tenth and above the ninetieth percentiles. The line style denoted for each land cover type is the same for Figures 2b and 2d. Local time in the SSA and NSA is 6 hours less than UTC.

summer EF is higher in the SSA than the NSA for all four paired sites, fen, old black spruce, old jack pine and young jack pine, although the difference is a little less clear than in Figure 2 (see section 3.2).

3.2. Diurnal Cycle of Evaporative Fraction and Surface Conductance

Figure 2 compares the diurnal cycles (an average from May 24 to September 19, 1994, corresponding essentially to the growing season) of (1) air temperature and relative humidity, (2) evaporative fraction, (3) solar and net radiation, and (4) surface conductance for the BOREAS flux sites in the SSA and NSA. As in Figure 1, the meteorological variables are averaged over all sites. Figure 2a shows an afternoon maximum of temperature and a minimum of RH. Figure 2b shows a daytime minimum of EF at all sites, with EF at the SSA exceeding EF at the NSA for each paired land cover. In addition, Figure 2b shows characteristically different diurnal patterns of EF for each land cover type, independent of geographic location. At the fen sites, EF increases as RH falls from an early morning maximum to a midafternoon minimum. At the aspen and old black spruce sites, EF is relatively constant during the midday hours. At the jack pine sites, EF falls the most and reaches the lowest afternoon minimum. These differences reflect the decreasing availability of water for evaporation and transpiration and the strongest stomatal control on transpiration at the jack pine

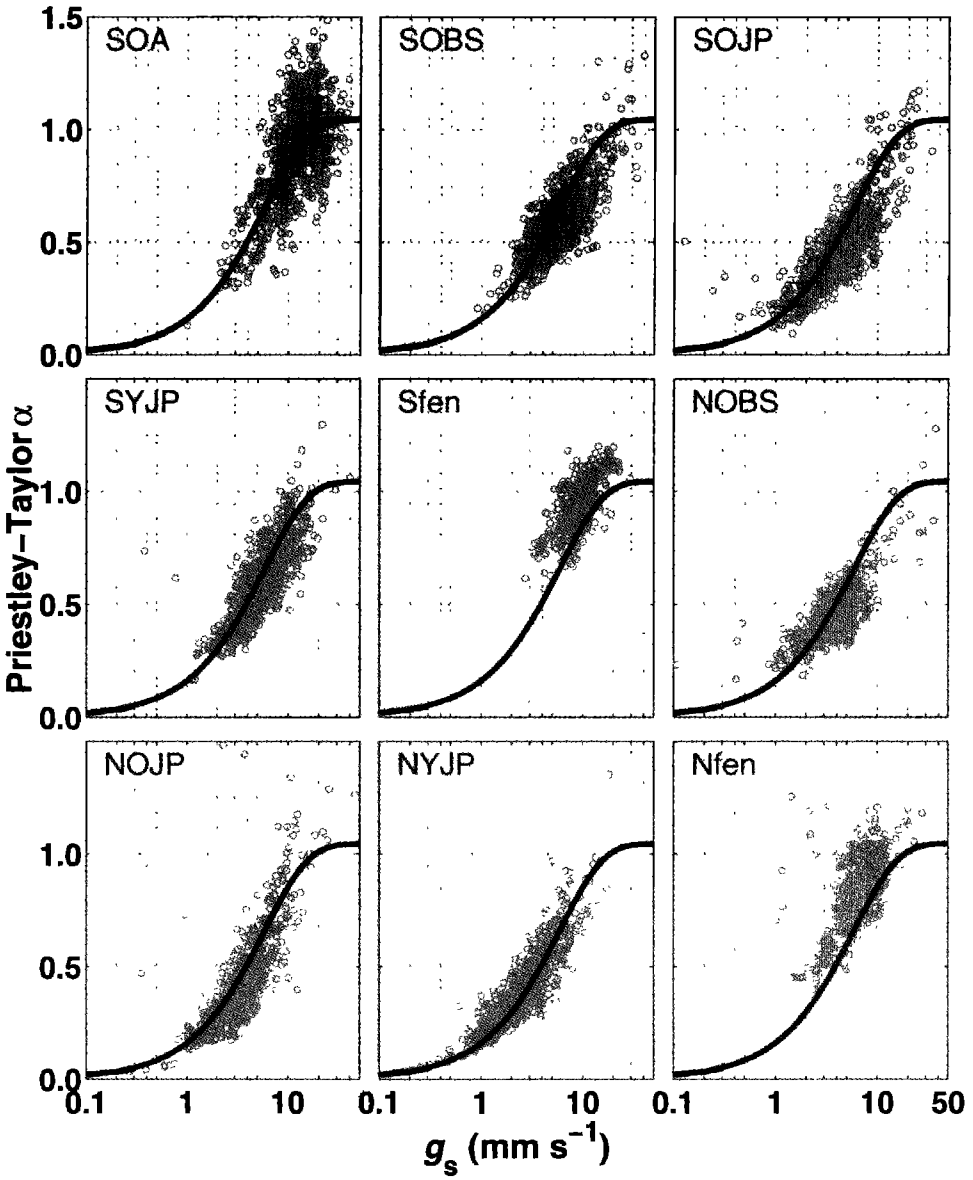

Figure 3. Half-hourly values of the Priestley-Taylor coefficient α as a function of the surface conductance to water vapor g_s for the BOREAS tower flux sites on May 24 to September 19, 1994. The plots show measured data only (i.e., with no gap filling). Data are excluded for solar irradiances < 500 W m^{-2}. The solid line is a landscape mean from equation (8), fit to the data from all sites.

sites. Mean RH is a little lower for the NSA than the SSA, consistent with the uniformly lower EF.

The SSA-NSA difference in EF is consistent with the earlier results of *Barr and Betts* [1997], who analyzed the boundary layer budgets of the BOREAS radiosondes. They reported mean midday Bowen ratios for the BOREAS NSA and SSA during the 1994 intensive field campaigns that correspond to evaporative fractions of 0.53 and 0.45, respectively. These values are intermediate between the lower conifer values and the higher aspen and fen values in Figure 2 and are ~30% higher than the mean midday values for mature black spruce (0.43 in the SSA and 0.34 in the NSA). These differences illustrate that although the boreal forest landscape is dominated by conifers, particularly black spruce [*Betts et al.*, this issue], its energy balance at the landscape scale is also significantly influenced by other land covers with higher evaporative fractions.

Figure 2c shows the mean diurnal cycles of solar and net radiation, and Figure 2d shows the derived surface conductance to water vapor. The SSA aspen site has the highest surface conductance, and the jack pine sites have the lowest. Unlike the fen sites, where conductance is nearly symmetric with radiation (more so in the north than in the south), the diurnal pattern of conductance is markedly asymmetric at the forest sites. The high forest conductances in the early morning to midmorning reflect the maximum daytime stomatal opening as a result of low-in-magnitude leaf water potentials, high RH, and low D [*Margolis and Ryan*, 1997]. At some sites and times they may also reflect the presence of early morning dew on the canopy. The fall of

conductance between midmorning and late afternoon at the forest sites reflects stomatal control as D increases [*Margolis and Ryan*, 1997].

As was observed with EF, the paired sites (fen, old black spruce, old jack pine, and young jack pine) each have higher mean conductance in the SSA than in the NSA. There is little difference in incoming short-wave radiation or in temperature between the NSA and SSA, and the 5% lower midday RH in the NSA is not sufficient to account for the significantly lower g_s. The higher rainfall in 1994 in the SSA may explain part of the higher conductance, particularly at the jack pine sites. However, *Betts et al.* [this issue] showed a similar difference between the black spruce sites in 1996, when rainfall was similar in both SSA and NSA, so we doubt that the seasonal atmospheric and soil water constraints between south and north are entirely responsible for the lower surface conductance in the north. Other possibilities include differences in nitrogen availability and leaf area index.

3.3. Coupling of Alpha to Surface Conductance

Figure 3 shows half-hourly values of the Priestley-Taylor coefficient α (equation 2) as a function of g_s (equation 5) for each of the nine sites. The scale for g_s is logarithmic. The solid line in each plot shows the mean relationship between α and g_s for all sites, fit to a function suggested by *Monteith* [1995]:

$$\alpha = \alpha_m(1-\exp[-g_s/g_c]), \quad (8)$$

where α_m is the asymptotic limit for α and g_c is a scaling conductance. Note the tight coupling of α to g_s. For the data acceptance threshold of $R_s > 500$ W m^{-2} in Figure 3 the mean (all site) estimates for α_m and g_c (equation 8) are 1.05 and 6.0 mm s^{-1}, respectively, in reasonable agreement with *Monteith's* [1995] estimates of 1.1 to 1.4 for α_m and 5.0 mm s^{-1} for g_c. The estimate for g_c (but not α_m) is sensitive to the R_s threshold used to screen the data and drops to 4.6 mm s^{-1} for $R_s > 250$ W m^{-2}. Our estimate for α_m may be lower than Monteith's simply because his analysis included data from productive agricultural sites with higher values for α and g_s than the boreal sites in this study.

The general applicability of the mean (landscape) relationship from (8) at all sites shows the broad utility of relationships like (8). The paired sites (old black spruce, old jack pine, young jack pine, and fen) have very similar α-g_s relationships, independent of their geographic location. However, the individual land covers show subtle but consistent departures from the mean α-g_s relation. The average departures of α from the landscape mean (equation (8), shown as the solid lines in Figure 3) are +18% for fen, +4% for mature aspen, -1% for young jack pine, -9% for old black spruce, and −11% for old jack pine. If the α-g_s relationship is indeed universal as, for example, *de Bruin* [1983], *McNaughton and Spriggs* [1989] and *Monteith* [1995] argue, then these departures may show the impact of spatial heterogeneity on evapotranspiration from contrasting elements in a patchwork landscape. For patches like fen that are relatively wet and have above-average values for g_s and weak feedback from D to g_s, the surrounding drier patches act as sensible heat sources via horizontal advection [*McNaughton*, 1976]. This causes disequilibrium between g_s, λE and D. The above-equilibrium D enhances λE from the fen patches and causes α to be higher than that of an extensive fen. For patches like conifer with lower than average values for g_s, the horizontal advection of cooler, moister air from the surrounding wetter patches causes D to be lower than the equilibrium value. This diminishes λE and causes α to be lower than that of an extensive coniferous landscape. However, the resultant λE and α are also affected by the presence of a strong feedback from D to g_s in coniferous species. This feedback increases g_s above its equilibrium value and dampens the reductions in λE and α. The net effect of surface heterogeneity at the landscape scale is to heighten the differences in EF and α among contrasting land covers.

3.4. Impact of Energy Balance Closure

The analysis of section 3.3 has one caveat, which is related to the energy balance closure adjustments in section 2.2. With the exception of NOJP the sites with the largest energy closure adjustments to λE and g_s (the fens) also have the largest positive deviations of α from (8), whereas the sites with the smallest energy closure adjustments to λE and g_s (the mature conifers) have the largest negative deviations from (8). If we repeat the analysis in Figure 3 but substitute the unadjusted values for α and g_s, the contrasts between land covers diminish but do not disappear. The average departures of α from the landscape mean become +7% for fen, +2% for mature aspen, +1% for young jack pine, 0% for old black spruce, and −14% for old jack pine. Note that the paired sites continue to show consistent departures from the landscape mean and that the old black spruce sites now typify the boreal landscape. The revised values for α_m and g_c (equation 8) are 0.94 and 5.8 mm s^{-1}, respectively. This caveat tempers our conclusion about the significance of horizontal advection in a patchwork landscape, but it does not invalidate it. It also highlights the importance of careful measurement of Q_s and the need for a more fundamental understanding of the energy imbalance in eddy covariance studies.

4. Summary and Conclusions

This paper summarizes the sensible and latent heat flux data from the 1994 BOREAS tower flux sites and contrasts the southern and northern study areas and the behavior of five different land covers. The data show consistently higher evaporative fractions and surface conductances in the south than the north, with no obvious relation to climatic differences. The ranking of the evaporative fractions by land cover is, in order of largest to smallest, aspen, fen, black spruce, and jack pine. Land cover differences in EF are attributed in part to differences in surface conductance and stomatal control and in part to the impact of spatial heterogeneity on evapotranspiration from contrasting elements in a patchwork landscape. The coniferous and, especially, the jack pine ecosystems show the strongest stomatal control of transpiration. Both southern and northern study areas have a similar relationship between the Priestley Taylor coefficient α and surface conductance, but the relationship varies subtly among land covers. The variation may show how spatial heterogeneity in land cover and surface conductance at the landscape scale influences α among contrasting landscape elements. Spatial heterogeneity increases α from patches like fen and aspen with higher conductance and decreases α from coniferous patches with

lower conductance. We conclude that although conifers dominate the boreal forest landscape, other land covers with higher evaporative fractions also influence its energy balance at the landscape scale. In evaluating the role of boreal forest in the global climate system, it will be important to consider the patchy, mosaic character of the boreal landscape.

Appendix A: Filling Gaps in H^*, λE^*, and g_s Data

To fill gaps in the time series of H^*, λE^*, and g_s, we modeled g_s as $f(R_s, T_a, D)$ at each site, roughly following *Jarvis* [1976]:

$$g_s = m g_x f(R_s) f(T_a) f(D), \quad \text{(A1)}$$

with

$$f(R_s) = \frac{R_s}{b_R + R_s}, \quad \text{(A2a)}$$

$$f(T_a) = \left[\frac{T_a - T_n}{b_T - T_n}\right]\left[\frac{T_x - T_a}{T_x - b_T}\right]^{\frac{T_x - b_T}{b_T - T_n}}, \quad \text{(A2b)}$$

and using $f(D)$ from *Lohammer et al.* [1980] (cited by *Massman and Kaufmann* [1991]):

$$f(D) = \frac{1}{1 + b_D D}. \quad \text{(A2c)}$$

We added the parameter m in (A1) to account for seasonal variations in g_x. The values for T_n and T_x in (A2b) were fixed at 0° and 40 °C, respectively. The value $f(T_a)$ in (A2b) was set to zero when $T_a < T_n$ or $T_a > T_x$.

The parameters in (A2a)-(A2c) were fit for each site using measured R_s, D, T_a, and g_s, where g_s was derived from (5) based on λE^*, the energy closure adjusted value for λE (section 2.2). The parameter fitting was done (using MatLab,) in two steps. First, g_x, b_R, b_D, and b_T in (A2a)-(A2c) were estimated for each site based on all data from May to September 1994, with m set to 1.0. The regression excluded g_s data below the 1st and above the 99th percentiles. Second, the seasonal variation in m was estimated daily using a moving window of 10 days in length by linear regression of g_s versus $g_x f(R_s) f(T_a) f(D)$ The regression line was forced through the origin. Using $f(T_a)$ in the regression gave only minimal benefit, as also reported by *Wu et al.* [2000] and *Massman and Kaufmann* [1991)], but $f(T_a)$ was retained.

Estimates for missing values of H^* and λE^* were then calculated using (3) and the Penman-Monteith combination equation [*Monteith*, 1981]:

$$\lambda E^* = \frac{s(R_n - Q_s) + g_a \rho c_p D}{s + \gamma(1 + g_a / g_s)}. \quad \text{(A3)}$$

Note that the estimates of g_s (equation A1) that were used to estimate missing values of λE^* in (A3) were energy closure adjusted values, because the parameters in (A1) and (A2a)-(A2c) had been fit using values of g_s that were calculated from closure-adjusted measurements (λE^*, sections 2.2 and 2.3).

Acknowledgments. We acknowledge the BOREAS investigators and their colleagues who operated the tower flux sites and collected the flux data (Table 1). We also acknowledge the efforts of the personnel from the BOREAS Information System. The suggestions of three anonymous reviewers were constructive and helpful. Financial support was provided to Alan Betts by NASA under grant NAG5-7377 and by NSF under grant ATM-9988618. Craig Smith received support from the Climate Research Branch of the Meteorological Service of Canada and Environment Canada's Science Horizons program.

References

Anderson, D.E., R. Striegl, D. Baldocchi, and D. Stannard, The fluxes of CO_2 and water vapor measured above and within young and mature jack pine forests of central Canada, Paper presented at Interactive Environmental Effects on Forest Stands Workshop, Int. Union of For. Res. Organ., New Zealand, January 1995.

Baldocchi, D.D., C.A. Vogel, and B. Hall, Seasonal variation of energy and water vapor exchange rates above and below a boreal jack pine forest canopy, *J. Geophys. Res., 102*, 28,939-28,952, 1997.

Barr, A.G. and A.K. Betts, Radiosonde boundary-layer budgets above a boreal forest, *J. Geophys. Res., 102*, 29,205-29,212, 1997.

Barr, A.G., K.M. King, T.J. Gillespie, G. den Hartog, and H.H. Neumann, A comparison of Bowen ratio and eddy correlation sensible and latent heat flux measurements above deciduous forest, *Boundary Layer Meteorol., 71*, 21-41, 1994.

Betts, A.K., J.H. Ball, and J.H. McCaughey, Near-surface climate in the boreal forest, *J. Geophys. Res.*, this issue.

Black, T.A., et al., Annual fluxes of water vapor and carbon dioxide fluxes in and above a boreal aspen forest, *Global Change Biol., 2*, 101-111, 1996.

Blanken, P.D., T.A. Black, P.C. Yang, H.H. Neumann, Z. Nesic, R. Staebler, G. den Hartog, M.D. Novak, and X. Lee, Energy balance and canopy conductance of a boreal aspen forest: partitioning overstory and understory components, *J. Geophys. Res., 102*, 28,915-28,927, 1997.

Brutsaert, W., Evaporation into the Atmosphere, 299 pp., D. Reidel, Norwell, Mass., 1984.

de Bruin, H.A.R., A model for the Priestley-Taylor parameter α, *J. Clim. Appl. Meteorol., 22*, 572-580, 1983.

Fitzjarrald, D.R., K.E. Moore, R.K. Sakai, and J. M. Freedman, Assessing the impact of cloud cover on carbon uptake in the northern boreal forest, *Trans. AGU*, 76(17), Spring Meet. S125, 1995.

Goulden, M.L., B.C. Daube, S.-M. Fan, D.J. Sutton, A. Bazzaz, J.W. Munger, and S.C. Wofsy, Physiological responses of a black spruce forest to weather, *J. Geophys. Res., 102*, 28,987-28,996, 1997.

Jarvis, P. G., J. M. Massheder, S. E. Hale, J. B. Moncrieff, M. Rayment, and S. L. Scott, Seasonal variation of carbon dioxide, water vapor, and energy exchanges of a boreal black spruce forest, *J. Geophys. Res., 102*, 28,953-28,966, 1997.

Jarvis, P.J, The interpretation of the variations in leaf water potential and stomatal conductance found in canopies in the field, *Philos. Trans. R. Soc. London, Ser. B. 273*, 593-610, 1976.

Lafleur, P. M., J. H. McCaughey, D.W. Joiner, P.A. Bartlett, and D.E. Jelinski, Seasonal trends in energy, water, and carbon dioxide fluxes at a northern boreal wetland, *J. Geophys. Res., 102*, 29,009-29,020, 1997.

Lohammer, T., S. Larsson, S. Linder, and Falk, O, FAST – simulation models of gaseous exchange in Scots pine, *Ecol. Bull. 32*, 505-523, 1980.

Mahrt, L., Flux sampling errors from aircraft and towers, *J. Atmos. Oceanic Technol. 15*. 416-429, 1998.

Margolis, H.A. and M.G. Ryan, A physiological basis for biosphere-atmosphere interactions in the boreal forest: an overview, *Tree Physiol., 17*. 491-499, 1997.

Massman, W.J. and M.R Kaufmann, Stomatal response to certain environmental factors: A comparison of models for subalpine trees in the Rocky Mountains, *Agric. For. Meteorol., 54*, 155-167, 1991.

McCaughey, J.H., P.M. Lafleur, D.W. Joiner, P.A. Bartlett, A.M. Costello, D.E. Jelinski, and M.G. Ryan, Magnitudes and seasonal patterns of energy, water, and carbon exchanges at a boreal young jack pine forest in the BOREAS northern study area., *J. Geophys Res., 102*, 28997-29007, 1997.

McNaughton, K.G., Evaporation and advection II: evaporation downwind of a boundary separating regions having different

surface resistances and available energies. *Q. J. R. Meteorol. Soc., 10,* 193-202, 1976.

McNaughton, K.G. and T.W. Spriggs, An evaluation of the Priestley and Taylor equation, *Estimation of Areal Evapotranspiration, IAHS Publ., 177,* 89-104, 1989.

Monteith, J.L., Evaporation and surface temperature, *Q. J. R. Meteorol. Soc., 107,* 1-27, 1981.

Monteith, J.L., Accommodation between transpiring vegetation and the convective boundary layer, *J. Hydrol., 166,* 251-263, 1995.

Newcomer J., et al. (Eds,), *Collected Data of The Boreal Ecosystem-Atmosphere Study*, [CD-ROM], NASA, Greenbelt, Md., 2000.

Ohmura, A., Objective criteria for rejecting data for Bowen ratio flux calculations, *J. Appl. Meteorol., 21,* 595-598, 1982.

Priestley, C.H.B. and R.J. Taylor, On the assessment of surface heat flux and evaporation using large-scale parameters, *Mon. Weather Rev., 100,* 81-92, 1972.

Sellers, P.J., et al., The Boreal Ecosystem-Atmosphere Study (BOREAS): an overview and early results from the 1994 field year, *Bull. Am. Meteorol. Soc., 77,* 1549-1577, 1995.

Sellers, P.J., et al., BOREAS in 1997. Experiment overview, scientific results, and future directions, *J. Geophys. Res., 102,* 28,731-28,769, 1997.

Suyker, A.E., S.B. Verma, and T.J. Arkebauer, Season-long measurement of carbon dioxide exchange in a boreal fen, *J. Geophys. Res., 102,* 29,021-29,028, 1997.

Thom, A., Momentum, mass and heat exchange of vegetation, *Q. J. R. Meteorol. Soc., 98,* 124-134, 1972.

Twine, T.E., W.P. Kustas, J.M. Norman, D.R. Cook, P.R. Houser, T.P. Meyers, J.H. Preuger, P.J. Starks, and M.L. Wesely, Correcting eddy-covariance flux underestimates over a grassland, *Agric. For. Meteorol., 103,* 279-300, 2000.

Verma, S.B., Aerodynamic resistances to transfers of heat, mass and momentum, *Estimation of Areal Evapotranspiration, IAHS Publ., 177,* 13-20, 1989.

Wu, A., T.A. Black, D.L. Verseghy, P.D. Blanken, M.D. Novak, W. Chen, and P.C. Yang, A comparison of parameterizations of canopy conductance of aspen and Douglas-fir forests by CLASS, *Atmos. Ocean, 38,* 81-112, 2000.

A. G. Barr and C. D. Smith, Meteorological Service of Canada, 11 Innovation Blvd., Saskatoon, Saskatchewan, Canada S7N 3H5. (alan.barr@ec.gc.ca; craig.smith@ec.gc.ca.)

A. K. Betts, Atmospheric Research, RR 3 Box 3125, 58 Hendee Lane, Pittsford, VT 05763. (akbetts@aol.com.)

T. A. Black, Faculty of Agricultural Sciences, University of British Columbia, 139-2357 Main Mall, Vancouver, British Columbia, Canada V6T 1Z4. (ablack@interchange.ubc.ca.)

J. H. McCaughey, Department of Geography, Queen's University, Kingston, Ontario, Canada K7L 3N6. (mccaughe@post.queensu.ca.)

(Received September 22, 2000; revised January 9, 2001; accepted January 26, 2001.)